

# Analysis of an Automated Machine Learning Approach in Brain Predictive Modelling: A data-driven approach to Predict Brain Age from Cortical Anatomical Measures

Jessica Dafflon<sup>\*1</sup>, Walter H. L. Pinaya<sup>2,3</sup>, Federico Turkheimer<sup>1</sup>, James H. Cole<sup>1</sup>, Robert Leech<sup>1</sup>, Mathew A. Harris<sup>4</sup>, Simon R. Cox<sup>5,6</sup>, Heather C. Whalley<sup>4</sup>, Andrew M. McIntosh<sup>4</sup> and Peter J. Hellyer<sup>†1</sup>

<sup>1</sup>*Department of Neuroimaging, Institute of Psychiatry, Psychology and Neuroscience, King's College London, UK*

<sup>2</sup>*Department of Psychosis Studies, Institute of Psychiatry, Psychology and Neuroscience, King's College London, UK*

<sup>3</sup>*Center of Mathematics, Computation and Cognition, Universidade Federal do ABC, Brazil*

<sup>4</sup>*Division of Psychiatry, University of Edinburgh, UK*

<sup>5</sup>*Lothian Birth Cohorts group, Department of Psychology, University of Edinburgh, UK*

<sup>6</sup>*Scottish Imaging Network, A Platform for Scientific Excellence (SINAPSE) Collaboration, Edinburgh, UK*

October 9, 2019

## Abstract

The use of machine learning (ML) algorithms has significantly increased in neuroscience. However, from the vast extent of possible ML algorithms, which one is the optimal model to predict the target variable? What are the hyperparameters for such a model? Given the plethora of possible answers to these questions, in the last years, automated machine learning (autoML) has been gaining attention. Here, we apply an autoML library called TPOT which uses a tree-based representation of machine learning pipelines and conducts a genetic-programming based approach to find the model and its hyperparameters that more closely predicts the subject's true age. To explore autoML and evaluate its efficacy within neuroimaging datasets, we chose a problem that has been the focus of previous extensive study: brain age prediction. Without any prior knowledge, TPOT was able to scan through the model space and create pipelines that outperformed the state-of-the-art accuracy for Freesurfer-based models using only thickness and volume information for anatomical structure. In particular, we compared the performance of TPOT (mean accuracy error (MAE):  $4.612 \pm .124$  years) and a Relevance Vector Regression (MAE  $5.474 \pm .140$  years). TPOT also suggested interesting combinations of models that do not match the current most used models for brain prediction but generalise well to unseen data. AutoML showed promising results as a data-driven approach to find optimal models for neuroimaging applications.

**Keywords** predictive modelling · automated machine learning · age prediction · neuroimaging

---

\*jessica.dafflon@kcl.ac.uk

†peter.hellyer@kcl.ac.uk

# 1 Introduction

The last few decades have seen significant progress in neuroimaging methodologies and techniques focused on identifying structural and functional features of the brain associated with behaviour. These methods, have been widely applied to assess differences at a group level between, for example, clinical groups. However, group-level statistics are limited and fail to make inferences that are applicable to the individual. With the advance of machine learning (ML) algorithms and their increased application in neuroimaging, the field is rapidly becoming more focused on exploring relationships between individual difference and behaviour, as well as, developing clinically relevant biomarkers of disorders (Pereira et al., 2009; Liem et al., 2017; Glaser et al., 2019; Yarkoni and Westfall, 2017; Bzdok and Ioannidis, 2019).

This recent shift was mainly due to the use of predictive modelling approaches, consisting of using ML algorithms to learn patterns from features in a dataset and to build an accurate model to predict an independent variable of interest in unseen data. However, choosing a model which is unsuitable for the statistical distribution the underlying data leads to significant problems with *over*-estimation of the model and loss of generalisation. Secondly, the sheer *mass* of learning approaches that are available with a vast array of different properties provides a bewildering set of choices for the practitioner; each with advantages and disadvantages both in terms of generalisation and computational complexity. This issue results in the occurrence of both type I and II errors, simply as a result of picking an inappropriate analysis technique for the underlying data. This is particularly problematic as new fields adopt machine learning approaches, and the choice of the methodology is often based on applications in other fields where data may have quite different statistical properties - or indeed simply be the product of whichever technique is currently in the zeitgeist.

The *no free lunch principle* (Wolpert and Macready, 1997) applied to ML, suggests that there are no single estimator and parameter combinations that will always perform well on every dataset. The selection of preprocessing steps, the choice of the algorithm, the selection of features and the model's hyperparameters are crucial and will vary with the task and data. Hence, the optimal application of ML technology requires the answer to at least three questions: What are the necessary preprocessing steps that should be performed to prepare the data? Is there a way of reducing the feature space to only the relevant features? Among the many available ML algorithms which one is the most appropriate for the data under analysis? That these choices are often arbitrary and defined only on *prior*-wisdom, is a challenge for neuroimaging which continues to face a significant replication crisis (Open Science Collaboration, 2015).

ML algorithms vary greatly in both their properties, complexity and the assumptions they make about the data they are applied to. They can be linear, non-linear and optimise different functions to predict continuous (regression) or categorical (classification) variables. Moreover, the performance of all ML algorithms depends on the fine-tuning of its hyperparameters (Jordan and Mitchell, 2015). In addition, feature extraction and feature selection methods are often used in series to reduce or enhance data complexity during the preprocessing stages of analysis. The consequence is that there are potentially infinite combinations of approaches that can be taken to identify relationships out of data. To cut through this complexity requires the development of tools that can automatically select the appropriate (combination of) preprocessing and ML techniques to apply to a dataset to

highlight relationships that are both generalisable and computationally efficient.

In recent years, automated machine learning (autoML) has been gaining attention. The aim of autoML is to take advantage of complexity in the underlying dataset to help guide and identify the most appropriate model (and their associated hyperparameters), optimising performance, whilst simultaneously attempting to maximise the reliability of resulting predictions. In this context, many different autoML libraries have been developed. Auto-WEKA (Thornton et al., 2013), Auto-Sklearn (Feurer et al., 2015) and Tree-based Pipeline Optimisation Tool (TPOT) (Olson et al., 2016a) are just a few examples. While the first two implement a hierarchical Bayesian method, the latter uses a tree-based genetic programming algorithm. Due to its user-friendly interface and the pipeline flexibility offered by the optimisation of a tree-based approach (Hutter et al., 2019), we have chosen to evaluate TPOT’s performance on this problem. The main idea behind the tree-based genetic programming is to explore different pipelines (i.e. combination of different operators that perform features selection, feature generation and model analysis) for solving a classification or regression problem. This is done through a multi-generation approach, starting from a collection of *random* models. Based on the performance and reliability of predictions at each generation those with the highest performance will be *bred* (i.e. combined or crossed-over), whilst random *mutations* of these models are also introduced. Therefore combinations of models that maximise both performance and have lower complexity survive and the ‘best’ candidate pipeline yielded by TPOT will consist of a combination of models and preprocessing methods that are best suited to the relationship being probed. Figure 1 presents a high-level schematics of our approach.

In this paper, we explore the application of TPOT as an autoML approach to structural neuroimaging data. As a test-case, we evaluated its efficacy to predict chronological age using structural brain data. Ageing is one factor inducing major variability in brain structure. Grey matter atrophy, increase in the ventricle sizes, cortical thinning are a few examples of structures that alter while we age (Hogstrom et al., 2013; Cole and Franke, 2017). As age-related changes can be detected with structural magnetic resonance imaging (MRI) different machine learning models, have been trained to learn the relationship between age and brain structure (Franke et al., 2010; Aycheh et al., 2018; Cole et al., 2015; Liem et al., 2017; Valizadeh et al., 2017; Madan and Kensinger, 2018; Becker et al., 2018). The main idea behind brain age studies is to find discrepancies between the predicted and chronological age, which might be used as biomarkers (Cole and Franke, 2017). As brain-age prediction has been extensively studied and its accuracy can be evaluated against the reported model accuracies the existing brain-age corpus (Aycheh et al., 2018; Cole et al., 2017; Franke et al., 2010; Valizadeh et al., 2017), we used this problem to test the settings, validity and limitations of autoML for imaging applications in using a regression approach. In this study, we demonstrate that: (1) the model’s performance is highly dependent on the initial model population defined by the initial model pool passed as a configuration and the population size; (2) there is no single analysis model that predicts age with the highest performance from the underlying structural imaging data; (3) models suggested by TPOT outperforms relevance vector regressor (RVR), a state-of-the-art model used to predict brain age. Therefore, TPOT can be used as a data-driven approach to learn patterns in the data, to automatically select the best hyperparameters and models in a researcher unbiased fashion to avoid common pitfalls from ML algorithms such as overfitting.

## 2 Methods

### 2.1 Subjects and Datasets

In this analysis, T1-weighted MRI scans from N=10,307 healthy subjects (age range 18-89 years, mean age = 59.40) were obtained from 13 publicly available datasets where each dataset used one or more scanners to acquire the data. A summary of the demographics and imaging information can be found in Table S2 (for more details about the BANC dataset see (Cole et al., 2017)) and for the UK Biobank (Sudlow et al., 2015; Alfaro-Almagro et al., 2018) ([https://biobank.ctsu.ox.ac.uk/crystal/crystal/docs/brain\\_mri.pdf](https://biobank.ctsu.ox.ac.uk/crystal/crystal/docs/brain_mri.pdf)). From the original n=2001 subjects present on the BANC dataset, we only used 1227 subjects and excluded all subjects from the WUSL Cohort after performing Freesurfer quality control checks.

### 2.2 MRI Preprocessing

Using the recon-all pipeline in Freesurfer version v6.0 (Dale et al., 1999), individual T1-weighted MRI images were preprocessed and parcelled into 116 thickness and volume information for anatomical structures (for the full list of features see Table S3), according to the Desikan-Killiany atlas and ASEG Freesurfer atlas (Desikan et al., 2006). From these segmented regions, we extracted the cortical thickness and volume to be the input data for our further analysis.

### 2.3 TPOT Automated Analysis

TPOT (Olson et al., 2016b,a) uses genetic programming to search through different operators (i.e. preprocessing approaches, machine learning models, and their associated hyperparameters) to iteratively evolve the most suitable pipeline with high accuracy. It does so by 1) generating a pool of random analysis models sampled from a dictionary of preprocessing approaches and analysis models (See Table S1 for a list of the models used); 2) evaluating these models using 10-fold cross-validation, to identify the most accurate pipeline with the lowest amount of operators; 3) breeding the top 20 selected pipelines and applying local perturbations (e.g. mutation and cross-over); 4) re-evaluating the pipeline in the next generation. This process is repeated for a specified number of generations before settling on a final optimal pipeline that has high accuracy and low complexity (i.e., lowest number of pipeline operators). To make sure that the operators are combined in a flexible way, TPOT uses a tree-based approach. That means that every pipeline is represented as a tree where the nodes represented by the different operators. Every tree-based pipeline starts with one or more copies of the dataset and every time the data is passed through a node the resulting prediction is saved as a new feature. In particular, TPOT uses a genetic programming algorithm as implemented in the Python package DEAP (Fortin et al. (2012); for a more detailed description of the TPOT implementation see Olson et al. (2016a)).

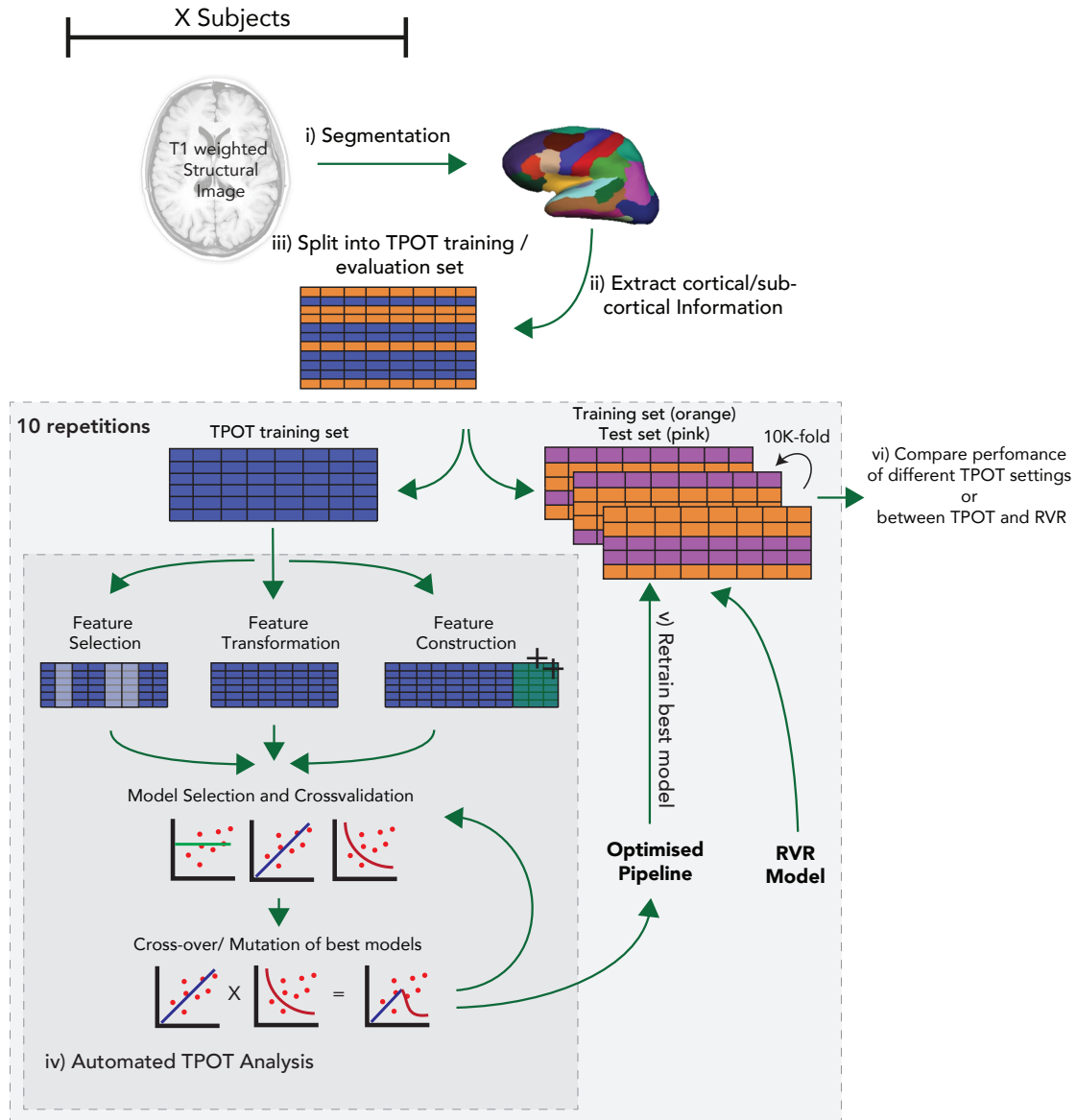


Figure 1: **Overview of experimental design:** The subject’s structural MRI is used to create a parcellation of cortical and subcortical regions. The dataset was split into 2 independent sets: TPOT training set and evaluation set. The TPOT training set was passed to TPOT, which depending on the specified configuration performed feature selection, feature transformation, feature generation, or a combination of those and evaluated the model’s performance. For each generation, a 10-fold cross-validation was performed and the best models for that specific generation were identified, crossed-over/mutated, and passed to the next generation. At the last generation, the pipeline with the lowest mean accuracy error was identified and returned by TPOT. We then retrained the optimised pipeline on the independent evaluation set and tested its performance using a 10-fold cross-validation. Finally, we compared the MAEs between different TPOT configurations and between TPOT and RVR.

### 2.3.1 Regression

**TPOT hyperparameters exploration** We used TPOT to find the 'best' pipelines to predict brain age, where the fitness of the pipeline is defined by a low MAE between the predicted and the subject's chronological age. To do this, we randomly selected 1546 subjects from the dataset (TPOT training set), and we applied TPOT on them for 10 generations to find the most fitted ML pipeline - the pipelines with the highest accuracy. The optimal pipeline suggested by TPOT was then used to train an independent (n=8761) dataset and its performance was evaluated using a 10-fold cross-validation. The TPOT analysis and the evaluation of the model in an independent training set was repeated 10 times. As a result, we obtained 100 performance scores for each configuration that were used to evaluate the impact of manipulating a) the types of model preprocessing, b) number of models tested on the first generation, and c) mutation and cross-over rate.

**Comparison between TPOT and RVR** We also performed a 10 times repetition with 10-fold cross-validation (as described above) to assess the difference in performance between the 'best' pipelines yielded by TPOT and the RVR, a standard model used in brain-age prediction (Franke et al., 2010; Madan and Kensinger, 2018; Kondo et al., 2015; Wang et al., 2014). In addition, to check if the underlying age distribution would have an effect on the models yielded by TPOT, we repeated the analysis using 784 subjects whose age was uniformly distributed between 18-77 years old. In this case, we used n=117 subjects to train TPOT and obtain the best pipeline. The remaining subjects (n=667) were used to train the best pipeline using a 10-fold cross-validation. Similarly to the other analyses, this evaluation process was also repeated 10 times resulting in 100 MAE values for each condition.

While a Student's t-test is often used to check the difference in performance between two models; Student's test assumes that samples are independent, an assumption that is violated when performing a k-fold cross-validation. As part of the k-fold cross-validation procedure, one subject will be used in the training set k-1 times. Therefore, the estimated scores will be dependent on each other, and there is a higher risk of type I error. For this reason, we used a corrected version of the t-test that accounts for this dependency (Nadeau and Bengio, 2000) when comparing the performance of TPOT and RVR and the Friedman test when comparing different hyperparameters from TPOT (Demšar, 2006).

## 3 Results

We firstly investigated which models survived through the different generations. Figure 2 shows the counts of the different models in one of the repetitions. Random Forests and Extra Trees Regressors are the most popular models followed by Elastic Nets. Decision Trees and K-Nearest Neighbours also have a high popularity for the feature selection configuration.

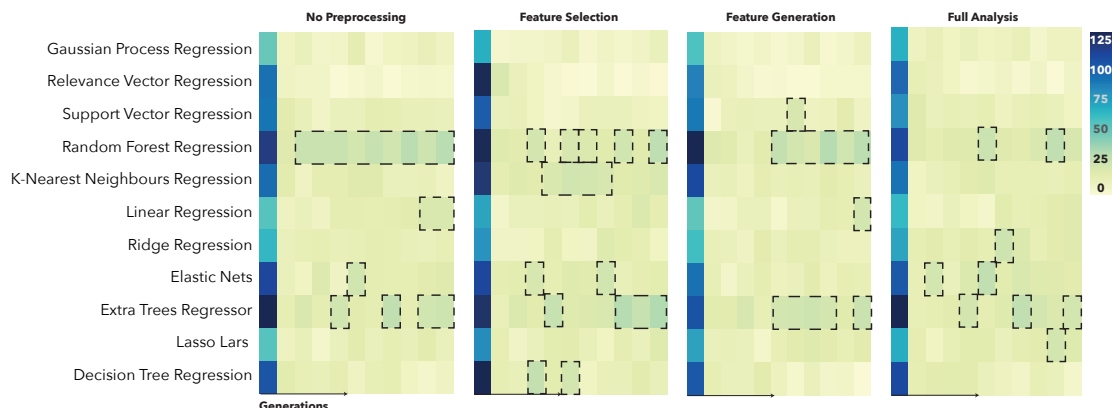


Figure 2: **Overview of the models count for each generation from one repetition for the different configurations experiments:** **A:** Models with a darker colour were more popular than models with lighter colour. Across the four experiments, Random Forest, K-Nearest Neighbours, Linear Regression and Extra Trees Regressors are the models with the highest count per generation. To make sure that all models were represented we increased the number of times the models were evaluated in the first generation.

### 3.1 TPOT parameter exploration

We then explored if the changes in the TPOT configuration are associated with a different performance (Figure 3B). We observed that independent of the preprocessing we chose the performance varied between 4.3 and 4.9 years. In addition to that, for every repetition TPOT found a different pipeline which was considered to be most accurate (Figure 3A). Similarly, we analysed the change in performance when varying the initial population of pipelines (Figure 3C). If a model was not selected on the initial population it will never be present in future generations, therefore we expected that a larger initial population would lead to a more diverse pool and therefore be associated with higher performances. We also explored the effect of mutation and crossover rate on the performance of the derived pipelines. For a combination of high (0.9), low (0.1), mid-ranges (0.5) mutation and cross-over rates. (Figure 3D). For all configurations, the performance of the best models yielded by TPOT oscillated between 4.3 and 4.9 years. These suggest that there is not one single model that best describes the dataset but a combination of many models leads to a higher performance and independent of the of the underlying data structure TPOT was able to a pipeline that yielded high performance.

### 3.2 Comparison between TPOT and RVR

To assess the efficacy of the TPOT approach applied to neuroimaging data, we compared the performance of the TPOT's pipelines using the Full Analysis configuration with Relevance Vector Regression. When using the entire dataset TPOT had a lower MAE and higher Pearson's Correla-

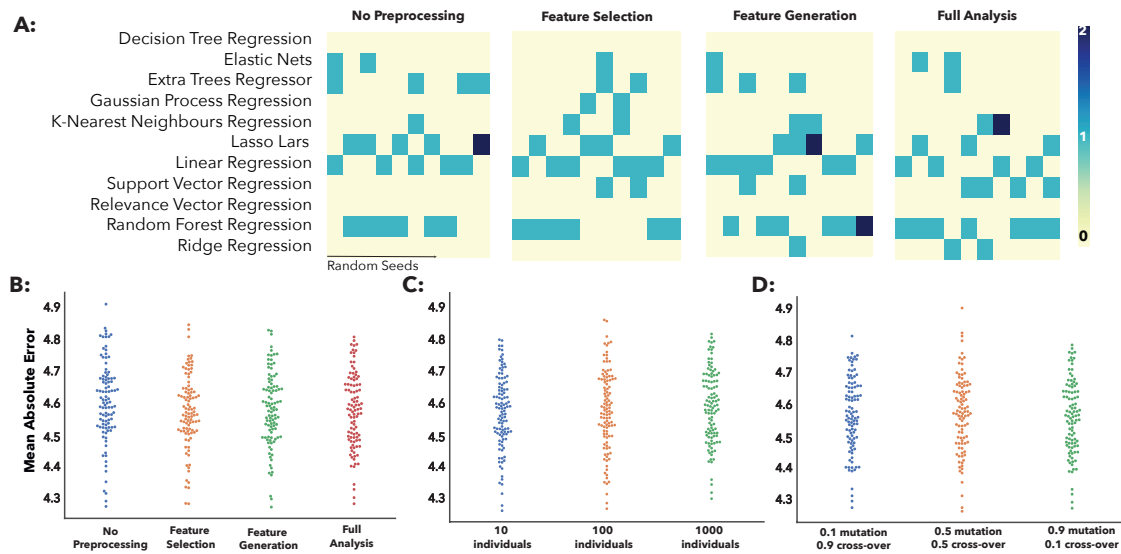


Figure 3: **Overview of the ensembles for the different analysis configurations at each repetition and their performance:** **A:** Schematic overview of the models composing the 'best' ensembles yielded by TPOT at each repetition. A darker colour represents models with higher counts. Random Forest Regression, Extra Trees Regressors, Lasso Lars and Linear Regression, were the most frequently represented. Despite the different models combinations among the different preprocessing analysis (**B:**), initial population size (**C:**), and mutation/cross-over rate (**D:**), there was no difference in the yielded performance.

	MAE	p-value	t	Pearson’s Correlation	p-value	t
TPOT	$4.612 \pm .124$	<b>&lt; .01</b>	-6.441	$.874 \pm .012$	<b>&lt; .01</b>	3.745
RVR	$5.474 \pm 0.140$			$.813 \pm .0102$		
TPOT (uniform distribution)	$5.594 \pm .0706$	<b>&gt; .5</b>	-.616	$.917 \pm .027$	<b>&gt; .5</b>	.007
RVR (uniform distribution)	$5.975 \pm .525$			$.919 \pm .013$		

Table 1: **Comparison between TPOT and RVR:** While TPOT has a significant higher accuracy and Pearson’s Correlation when using the original data distribution, when using the uniformly distributed dataset both models had a similar performance. (The values represent  $\pm SD$ ).

tion between true and predicted age (Figure 4). However, when we applied TPOT to a uniformly distributed dataset there was no significant difference between the models yielded by TPOT and RVR (Table 1). Nevertheless, the models suggested by TPOT using both datasets with the different age distribution were similar (Figure S1).

## 4 Discussion

The successful choice of an ML pipeline to predict variables of interest (such as age) from neuroimaging data is driven by the statistical characteristics and distribution of the dataset under analysis. In most cases, the choice of machine learning model applied in multivariate analysis of neuroimaging data is rather arbitrary - based on prior models that ‘have worked’, or by selecting whichever model is most novel in the eyes of the analysis community. To explore an alternative approach to model selection for a relatively simple problem, in this work, we investigated the application of an automated analysis technique: TPOT. The TPOT approach is a data-driven methodology which is agnostic to statistical model *and* preprocessing of the dataset - aiming to find the best pipeline available to fit the statistical properties of the underlying dataset, whilst simultaneously controlling for overfit and reliability. We showed that: (1) the performance of the models suggested by TPOT is highly dependent on the specified model pool (i.e. algorithms and hyperparameters) that TPOT has available to use. However, feature selection, feature generation, initial population size the mutation rate and cross-values rate do not have a substantial effect on the TPOT’s performance. (2) There is not one single machine learning algorithm that performs the best, but good performance is achieved by a combination of models. (3) The pipelines suggested by TPOT performed significantly better than commonly used methods when performing a brain age regression from brain MRI scans.

Commonly used algorithms to predict brain age include a combination of linear and non-linear ML algorithms such as: Multiple linear regression (Valizadeh et al., 2017), Gaussian Process Regressors (Cole et al., 2015; Becker et al., 2018), K-nearest neighbours (Valizadeh et al., 2017), Relevance Vector Regression (Wang et al., 2014; Valizadeh et al., 2017; Franke et al., 2010), Random Forests (Valizadeh et al., 2017) and Neural Networks (Cole et al., 2017; Valizadeh et al., 2017). In this study, we used an autoML approach that searched for the most accurate pipeline over a pool of the

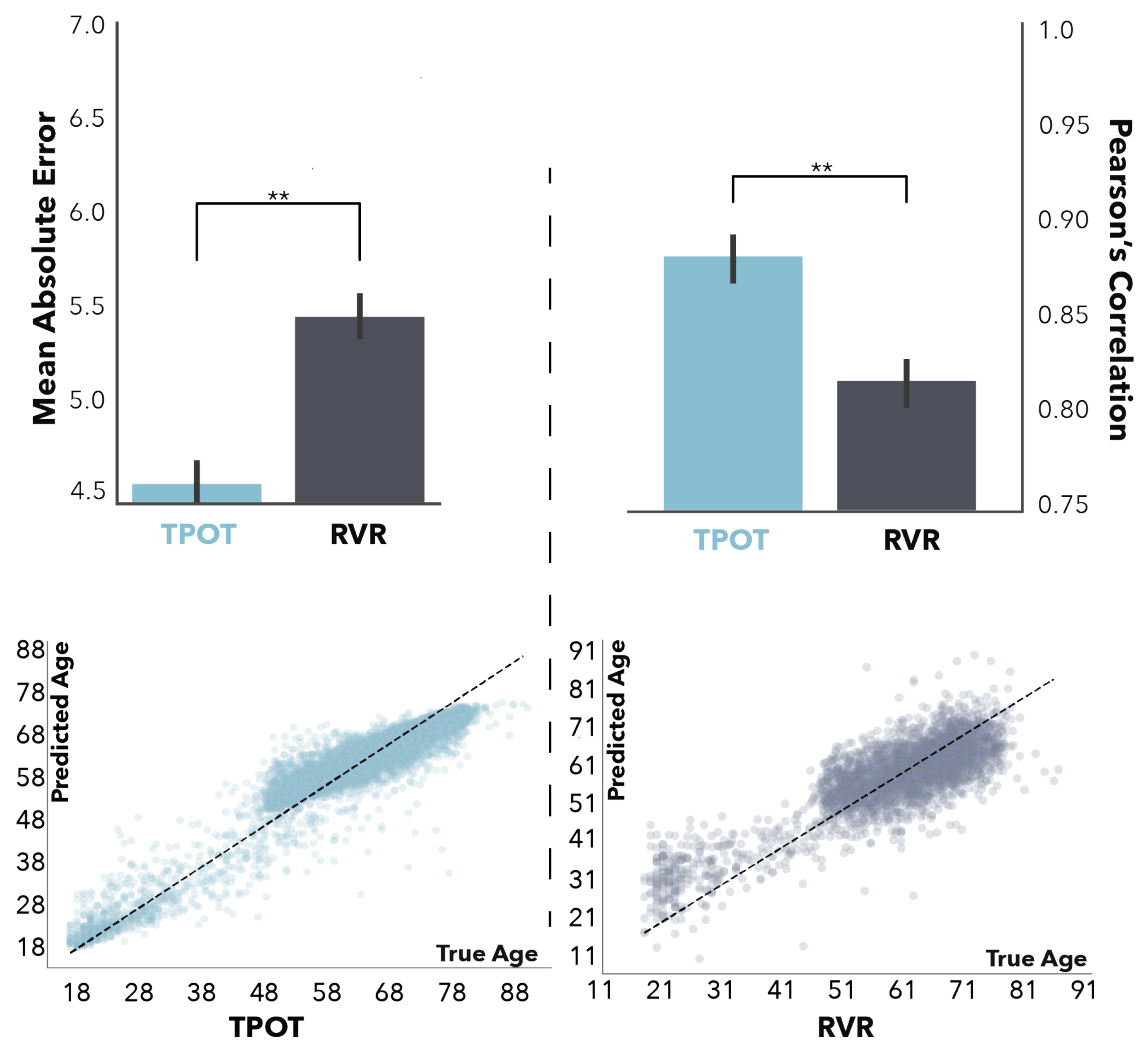


Figure 4: **Comparison of model's performance between TPOT and RVR:** We compared the MAE (top panel left) and Pearson's Correlation (top panel right) between True and Predicted age of the optimised model suggested by TPOT with and RVR on the test set. The lower panels show the Predicted vs the True age for one of the optimal pipelines suggested by TPOT (left) and RVR (right). Note that although both models use the same subject's to make prediction, the scales of the TPOT and RVR predictions are different, the RVR model predicts young subject's to be younger and old as older. Asterisks show differences that are statistically significant at  $p < 0.01$  (t-test corrected); Error bars indicate  $\pm 1SD$ .

commonly used algorithms and compared its performance to RVR. We observed that the variance in the predicted accuracy is very low on the test dataset for the pipelines suggested by TPOT but also for the RVR model. This suggests that the models are not fitting to noise but are finding interesting patterns in the data. Nevertheless, it is interesting to note that for every analysis’s repetition, a different pipeline was yielded by TPOT which had the lowest MAE (i.e. ‘best’ pipeline; Figure 3). This is likely because there exists no single model that always performs better for this type of regression problem. Similarly, when analysing age prediction using voxel-wise data Varikuti et al. (2018) previous work showed that the pattern of ‘important’ voxels is different across different training sets. Given the strength of the association between brain structure and age, and high levels of correlation between different brain regions, it seems that multiple different approaches can achieve high levels of prediction accuracy. This cautions against the over-interpretation of specific sets of model weights or coefficients as being those specifically important for brain ageing, as it seems that a different weighting on the brain could reach similar levels of performance. Inference on which brain regions are most associated with ageing is better conducted using a longitudinal within-subjects study design, rather than a multivariate predictive model such as those used in TPOT. Our results also highlight that all models yielded a similar MAE and were composed by a combination of linear and non-linear models (Random Forest Regression, Extra Tree Regression, K-Nearest Neighbours and Ridge or Lasso Regression; Figure 3 and Figure 2). In accordance with our results, Valizadeh et al. (2017) also reported similar brain-age prediction accuracy when comparing Random Forest and multiple linear regression. One of the main advantages of Random Forests is that it can deal with correlated predictors, while in a linear regression correlated predictors might bias the results. Therefore, by combining both algorithms in an ensemble, TPOT combines the strengths of both algorithms. Random forests have also been used by Liem et al. (2017) to combine multi-modal brain imaging data and generate brain-age prediction. In particular, Liem et al. (2017) used a Linear Support Vector Regression to predict age and stacked these models with Random Forests. This combined approach was able to improve brain-age prediction. Our interpretation of these observations is that the use of Random Forests and the hyperparameters found by TPOT ‘better fit’ the non-trivial non-linearities present in the dataset, transforming them within a n-dimensional manifold which can then be fed trivially into a linear classifier. A similar observation has been described by Aycheh et al. (2018), where a combination of Sparse Group Lasso and Gaussian process regression was used to predict brain age. On the other hand, whilst stable, and able to generalise, this non-linear transformation and combinations of different models into a pipeline makes interpretation of important features within the dataset impossible.

We also noted that when using a subsample of the dataset that has a uniform distribution, similar models were used by TPOT to build ensembles, nevertheless the difference in performance between TPOT and RVR was not significant (Table 1). We hypothesise that by using a uniform distribution we make the problem of age regression easier and therefore obtained similar performance between the TPOT and RVR approach, or that the reduced sample used to pre-train TPOT was not sufficient to obtain an accurate fit. It would be interesting for future research to explore these hypotheses further.

In the context of other literature, it is important to note that more accurate brain-age prediction models (Cole et al., 2017), do exist. As shown by Cole et al. (2017), Convolutional Neural Networks can predict brain age with a MAE of 4.16 years using a similar age range (18-90 years, mean age=36.95). As developing neural networks requires in-depth knowledge of architecture engineering,

it would be interesting to use autoML approaches to explore and select the most appropriate network architecture. However, the approach in the present study does not make any assumptions about the underlying statistics of the dataset and does not require any fine-tuning of the model of choice but still achieve state-of-the-art accuracy. When comparing the accuracy of different studies, it is important to take into account the age range of the analysed sample, as age prediction in a small range has less variability than in a large range. In fact, using a sample with subjects aged 45-91 Aycheh et al. (2018) obtained a MAE of 4.02 years. While Valizadeh et al. (2017) had a similar age range as that described in our project, they do not report the MAE for the entire sample and use instead 3 age groups (8-18 years, 18-65 and 65-96 years) to test the accuracy of different models. In general, Valizadeh et al. (2017) reported lower accuracy for the older group with MAE ranging between 4.90 and 14.23 years, when using only the thickness information. On the other hand, Liem et al. (2017) using only the cortical thickness reported a MAE of 5.95 years (analysed age range 18 - 89 years, mean = 58.68).

In the specific case of Deep-Neural Network approaches to the brain age problem, whilst improvements can be made on the accuracy of the model, often this is at the cost of reliability. As TPOT can accommodate a wider set of models, it would be interesting to include Neural Networks on the model pool and compare its performance against the range of selected models or to use other autoML toolboxes like autokeras (Jin et al., 2019) or Efficient Neural Architecture Search via Parameter Sharing (Pham et al., 2018). This automated approach will allow an extensive search of models and parameters and might also shed light into the question if deep learning is beneficial neuroimaging analysis. Recently, Schulz et al. (2019) showed that linear, kernels and deep learning models show very similar performance in brain-imaging datasets. Combining the potential power of deep-learning with a model-agnostic technique such as employed by TPOT, offers an potentially interesting route for further research.

## 5 Conclusion

Overall, our results show that the TPOT approach can be used as a data-driven approach to find ML models that accurately predict brain age. The models yielded by TPOT were able to generalise to unseen dataset and had a significantly better performance than RVR. This suggests that the autoML approach is able to adapt efficiently to the statistical distribution of the data. Although more accurate brain-age prediction models have been reported (Cole et al., 2017), the approach in the present study uses a wide age range (18-89 years old), uses only cortical anatomical measures, but most of all, it does not make any assumptions about the underlying statistics of the dataset and does not require any fine-tuning of the model of choice. By extensively testing different models and its hyperparameters, TPOT will suggest the optimal model for the training dataset. This approach removes possible introduced bias out of the loop and allows decisions about the model to be made in an automated, data-driven and reliable way.

## 6 Acknowledgements

We thank Sebastian Popescu for his help in carrying out the Freesurfer analysis on the BANC dataset, and Pedro F. da Costa for enlightening discussions and feedback on the analysis.

JD is funded by the Kings College London & Imperial College London EPSRC Centre for Doctoral Training in Medical Imaging (EP/L015226/1). WHLP was supported by Wellcome Trust (208519/Z/17/Z). FET is funded by the PET Methodology Program Grant (Ref G1100809/1) and the project grant Development of quantitative CNS PET imaging probes for the glutamate and GABA systems from the Medical Research Council UK (MR/K022733/1). SRC was supported by the Medical Research Council (MR/M013111/1 and MR/R024065/1), the Age UK-funded Disconnected Mind project (<http://www.disconnectedmind.ed.ac.uk>), and by a National Institutes of Health (NIH) research grant (R01AG054628). PJH is supported by a Sir Henry Wellcome Postdoctoral Fellowship from the Wellcome Trust (WT/106092/Z/14/Z)

**Author contribution** : JD, WHLP, FT, JHC, RL, PJH designed the study. MAE, SRC, HCW, AMM, JHC preprocessed the dataset. JD performed the experiments. JD, WHLP and PJH analysed the data. JD, PJH, WHLP, FT, JHC, SRC, HCW wrote and edited the manuscript.

## References

- F. Alfaro-Almagro, M. Jenkinson, N. K. Bangerter, J. L. R. Andersson, L. Griffanti, G. Douaud, S. N. Sotiropoulos, S. Jbabdi, M. Hernandez-Fernandez, E. Vallee, D. Vidaurre, M. Webster, P. McCarthy, C. Rorden, A. Daducci, D. C. Alexander, H. Zhang, I. Dragonu, P. M. Matthews, K. L. Miller, and S. M. Smith. Image processing and quality control for the first 10,000 brain imaging datasets from uk biobank. *Neuroimage*, 166:400–424, 02 2018. doi: 10.1016/j.neuroimage.2017.10.034.
- H. M. Aycheh, J.-K. Seong, J.-H. Shin, D. L. Na, B. Kang, S. W. Seo, and K.-A. Sohn. Biological brain age prediction using cortical thickness data: A large scale cohort study. *Front Aging Neurosci*, 10:252, 2018. doi: 10.3389/fnagi.2018.00252.
- B. G. Becker, T. Klein, C. Wachinger, A. D. N. Initiative, et al. Gaussian process uncertainty in age estimation as a measure of brain abnormality. *NeuroImage*, 175:246–258, 2018.
- D. Bzdok and J. P. A. Ioannidis. Exploration, inference, and prediction in neuroscience and biomedicine. *Trends Neurosci*, 42(4):251–262, Apr 2019. doi: 10.1016/j.tins.2019.02.001.
- J. H. Cole and K. Franke. Predicting age using neuroimaging: Innovative brain ageing biomarkers. *Trends Neurosci*, 40(12):681–690, 12 2017. doi: 10.1016/j.tins.2017.10.001.
- J. H. Cole, R. Leech, D. J. Sharp, and A. D. N. Initiative. Prediction of brain age suggests accelerated atrophy after traumatic brain injury. *Annals of neurology*, 77(4):571–581, 2015.

- J. H. Cole, R. P. Poudel, D. Tsagkrasoulis, M. W. Caan, C. Steves, T. D. Spector, and G. Montana. Predicting brain age with deep learning from raw imaging data results in a reliable and heritable biomarker. *NeuroImage*, 163:115–124, 2017.
- A. M. Dale, B. Fischl, and M. I. Sereno. Cortical surface-based analysis: I. segmentation and surface reconstruction. *Neuroimage*, 9(2):179–194, 1999.
- J. Demšar. Statistical comparisons of classifiers over multiple data sets. *Journal of Machine learning research*, 7(Jan):1–30, 2006.
- R. S. Desikan, F. Ségonne, B. Fischl, B. T. Quinn, B. C. Dickerson, D. Blacker, R. L. Buckner, A. M. Dale, R. P. Maguire, B. T. Hyman, M. S. Albert, and R. J. Killiany. An automated labeling system for subdividing the human cerebral cortex on mri scans into gyral based regions of interest. *Neuroimage*, 31(3):968–80, Jul 2006. doi: 10.1016/j.neuroimage.2006.01.021.
- M. Feurer, A. Klein, K. Eggensperger, J. Springenberg, M. Blum, and F. Hutter. Efficient and robust automated machine learning. In *Advances in neural information processing systems*, pages 2962–2970, 2015.
- F.-A. Fortin, F.-M. D. Rainville, M.-A. Gardner, M. Parizeau, and C. Gagné. Deap: Evolutionary algorithms made easy. *Journal of Machine Learning Research*, 13(Jul):2171–2175, 2012.
- K. Franke, G. Ziegler, S. Klöppel, C. Gaser, and Alzheimer’s Disease Neuroimaging Initiative. Estimating the age of healthy subjects from t1-weighted mri scans using kernel methods: exploring the influence of various parameters. *Neuroimage*, 50(3):883–92, Apr 2010. doi: 10.1016/j.neuroimage.2010.01.005.
- J. I. Glaser, A. S. Benjamin, R. Farhoodi, and K. P. Kording. The roles of supervised machine learning in systems neuroscience. *Prog Neurobiol*, 175:126–137, Apr 2019. doi: 10.1016/j.pneurobio.2019.01.008.
- L. J. Hogstrom, L. T. Westlye, K. B. Walhovd, and A. M. Fjell. The structure of the cerebral cortex across adult life: age-related patterns of surface area, thickness, and gyrification. *Cereb Cortex*, 23(11):2521–30, Nov 2013. doi: 10.1093/cercor/bhs231.
- F. Hutter, L. Kotthoff, and J. Vanschoren. Automated machine learning. *The Springer Series on Challenges in Machine Learning*, 2019. ISSN 2520-1328. doi: 10.1007/978-3-030-05318-5. URL <http://dx.doi.org/10.1007/978-3-030-05318-5>.
- H. Jin, Q. Song, and X. Hu. Auto-keras: An efficient neural architecture search system. In *Proceedings of the 25th ACM SIGKDD International Conference on Knowledge Discovery & Data Mining*, pages 1946–1956. ACM, 2019.
- M. I. Jordan and T. M. Mitchell. Machine learning: Trends, perspectives, and prospects. *Science*, 349(6245):255–260, 2015.
- C. Kondo, K. Ito, K. Wu, K. Sato, Y. Taki, H. Fukuda, and T. Aoki. An age estimation method using brain local features for t1-weighted images. *Conf Proc IEEE Eng Med Biol Soc*, 2015:666–9, 08 2015. doi: 10.1109/EMBC.2015.7318450.

- F. Liem, G. Varoquaux, J. Kynast, F. Beyer, S. K. Masouleh, J. M. Huntenburg, L. Lampe, M. Rahim, A. Abraham, R. C. Craddock, et al. Predicting brain-age from multimodal imaging data captures cognitive impairment. *Neuroimage*, 148:179–188, 2017.
- C. R. Madan and E. A. Kensinger. Predicting age from cortical structure across the lifespan. *Eur J Neurosci*, 47(5):399–416, Mar 2018. doi: 10.1111/ejn.13835.
- C. Nadeau and Y. Bengio. Inference for the generalization error. In *Advances in neural information processing systems*, pages 307–313, 2000.
- R. S. Olson, N. Bartley, R. J. Urbanowicz, and J. H. Moore. Evaluation of a tree-based pipeline optimization tool for automating data science. In *Proceedings of the Genetic and Evolutionary Computation Conference 2016*, pages 485–492. ACM, 2016a.
- R. S. Olson, R. J. Urbanowicz, P. C. Andrews, N. A. Lavender, J. H. Moore, et al. Automating biomedical data science through tree-based pipeline optimization. In *European Conference on the Applications of Evolutionary Computation*, pages 123–137. Springer, 2016b.
- Open Science Collaboration. Psychology. estimating the reproducibility of psychological science. *Science*, 349(6251):aac4716, Aug 2015. doi: 10.1126/science.aac4716.
- F. Pereira, T. Mitchell, and M. Botvinick. Machine learning classifiers and fmri: a tutorial overview. *Neuroimage*, 45(1):S199–S209, 2009.
- H. Pham, M. Y. Guan, B. Zoph, Q. V. Le, and J. Dean. Efficient neural architecture search via parameter sharing. *arXiv preprint arXiv:1802.03268*, 2018.
- M.-A. Schulz, B. Yeo, J. Vogelstein, J. Mourao-Miranada, J. Kather, K. P. Kording, A. Richard, and D. Bzdok. Deep learning for brains?: Different linear and nonlinear scaling in uk biobank brain images vs. machine- learning datasets. *hal-02276649*, 2019.
- C. Sudlow, J. Gallacher, N. Allen, V. Beral, P. Burton, J. Danesh, P. Downey, P. Elliott, J. Green, M. Landray, B. Liu, P. Matthews, G. Ong, J. Pell, A. Silman, A. Young, T. Sprosen, T. Peakman, and R. Collins. Uk biobank: an open access resource for identifying the causes of a wide range of complex diseases of middle and old age. *PLoS Med*, 12(3):e1001779, Mar 2015. doi: 10.1371/journal.pmed.1001779.
- C. Thornton, F. Hutter, H. H. Hoos, and K. Leyton-Brown. Auto-weka: Combined selection and hyperparameter optimization of classification algorithms. In *Proceedings of the 19th ACM SIGKDD international conference on Knowledge discovery and data mining*, pages 847–855. ACM, 2013.
- S. A. Valizadeh, J. Hänggi, S. Mérellat, and L. Jäncke. Age prediction on the basis of brain anatomical measures. *Hum Brain Mapp*, 38(2):997–1008, 02 2017. doi: 10.1002/hbm.23434.
- D. P. Varikuti, S. Genon, A. Sotiras, H. Schwender, F. Hoffstaedter, K. R. Patil, C. Jockwitz, S. Caspers, S. Moebus, K. Amunts, C. Davatzikos, and S. B. Eickhoff. Evaluation of non-negative matrix factorization of grey matter in age prediction. *Neuroimage*, 173:394–410, 06 2018. doi: 10.1016/j.neuroimage.2018.03.007.
- J. Wang, W. Li, W. Miao, D. Dai, J. Hua, and H. He. Age estimation using cortical surface pattern combining thickness with curvatures. *Med Biol Eng Comput*, 52(4):331–41, Apr 2014. doi: 10.1007/s11517-013-1131-9.

- D. H. Wolpert and W. G. Macready. No free lunch theorems for optimization. *IEEE transactions on evolutionary computation*, 1(1):67–82, 1997.
- T. Yarkoni and J. Westfall. Choosing prediction over explanation in psychology: Lessons from machine learning. *Perspectives on Psychological Science*, 12(6):1100–1122, 2017.

## 7 Supplementary Info

Algorithms	Sklearn Implementation
<i>Feature Selection</i>	
Principle Component Analysis	PCA
Fast algorithm for Independent Component Analysis	FastICA
Select the p-values corresponding to Family-wise error rate	SelectFwe
Select features according to a percentile of the highest scores	SelectPercentile
Remove low-variance Features	VarianceThreshold
<i>Feature Generation</i>	
Agglomerate features	FeatureAgglomeration
<i>Regression</i>	
Elastic Net model with iterative fitting along a regularisation path	ElasticNetCV
Randomised Decision Trees on sub-samples of the dataset	ExtraTreesRegressor
k-Nearest Neighbours Regression	KNeighborsRegressor
Cross-validated Lasso using the LARS algorithm	LassoLarsCV
Linear Support Vector Regression	LinearSVR
Linear Least squares with l2 regularisation	Ridge
Random Forest Regressor	RandomForrestRegressor
Ordinary Least Squares Linear Regression	LinearRegression
Decision Tree Regressor	DecisionTreeRegressor
Gaussian process regression	GaussianProcessRegressors
Relevance Vector Regression	RVR

Table S1: List of used Feature Selection, Feature Generation and Regression Algorithms

Cohort	N	Age		Sex male/female	Repository details	Scanner (Field strength)	Scan	Voxel dimensions
		mean (SD)	range					
ABIDE (Autism Brain Imaging Data Exchange)	147	24.43 (4.89)	18-40	130/17	INDI	Various (all 3T)	MPRAGE	Various
Beijing Normal University	151	21.36 (1.95)	18-28	63/88	INDI	Siemens (3T)	MPRAGE	1.33x1.0x1.0
Berlin School of Brain & Mind	49	30.99 (7.08)	20-60	24/25	INDI	Siemens Tim Trio (3T)	MPRAGE	1.0x1.0x1.0
CADDementia	12	62.33 (6.26)	58-79	9/3	<a href="http://caddementia.grand-challenge.org">http://caddementia.grand-challenge.org</a>	GE Signa (3T)	3D IR-FSPGR	0.9x0.9x1.0
Cleveland Clinic	31	43.55 (11.14)	24-60	11/20	INDI	Siemens Tim Trio (3T)	MPRAGE	2.0x1.0x1.2
ICBM (International Consortium for Brain Mapping)	42	27.71 (5.75)	24-60	14/28	LONI IDA	Siemens Magnetom (1.5T)	MPRAGE	1.0x1.0x1.0
IXI (Information eXtraction from Images)	394	46.21 (16.11)	20-86	159/235	<a href="http://biomedic.doc.ic.ac.uk/brain-development">http://biomedic.doc.ic.ac.uk/brain-development</a>	Philips Intera (3T); Philips Gyroscan Intera (1.5T); GE Signa (1.5T)	T1-FFE; MPRAGE	0.9375x0.9375x1x1.2
MCIC (MIND Clinical Imaging Consortium)	92	32.33 (11.92)	18-60	63/29	COINS	Siemens Sonata/Trio (1.5/3T); GE Signa (1.5T)	MPRAGE; SPGR	0.625x0.625x1.5
MIRIAD (Minimal Interval Resonance Imaging in Alzheimer's Disease)	23	69.66 (7.18)	58-85	12/11	<a href="https://www.ucl.ac.uk/drc/research/miriad-scan-database">https://www.ucl.ac.uk/drc/research/miriad-scan-database</a>	GE Signa (1.5T)	3D IR-FSPGR	0.9375x0.9375x1x1.5
NEO2012 (Adelstein, 2011)	39	29.59 (8.38)	20-49	18/21	INDI	Siemens Allegra (3T)	MPRAGE	1.0x1.0x1.0
Nathan Kline Institute (NKI) / Rockland	151	41.92 (18.24)	18-85	94/57	INDI	Siemens Tim Trio (3T)	MPRAGE	1.0x1.0x1.0
OASIS (Open Access Series of Imaging Studies)	61	42.82 (20.42)	18-89	20/41	<a href="http://www.oasis-brains.org/">http://www.oasis-brains.org/</a>	Siemens Vision (1.5T)*	MPRAGE	1.0x1.0x1.25
TRAIN-39	36	22.77 (2.52)	18-28	10/25	INDI	Siemens Allegra (3T)	MPRAGE	1.33x1.33x1.3
UK BIOBANK	9080	62.45 (7.48)	45-79	4334/4746	<a href="https://biobank.ctsu.ox.ac.uk/crystal/crystal/docs/brain_mri.pdf">https://biobank.ctsu.ox.ac.uk/crystal/crystal/docs/brain_mri.pdf</a>	Siemens Skyra (3T)	MPRAGE	1.0x1.0x1.0
<b>Training set total</b>	<b>10307</b>	<b>59.40 (12.33)</b>	<b>18-89</b>	<b>4961/5346</b>	-	-	-	-

INDI = International Neuroimaging Data-sharing Initiative ([http://fcon\\_1000.projects.nitrc.org](http://fcon_1000.projects.nitrc.org))  
COINS = Collaborative Informatics and Neuroimaging Suite (<http://coins.mrn.org>)  
LONI = Laboratory of Neuro Imaging Image & Data Archive (<https://ida.loni.usc.edu>)  
ABIDE consortiums comprising data from various sites with different scanners/parameters  
\*OASIS scans were acquired four times and then averaged to increase signal-to-noise ratio.

Table S2: Overview of the demographics and imaging parameters for the different datasets.

Table S3: List of used Freesurfer features

---

lh bankssts thickness	lh caudalanteriorcingulate thickness	lh caudalmiddlefrontal thickness
lh cuneus thickness	lh entorhinal thickness	lh fusiform thickness
lh inferiorparietal thickness	lh inferiortemporal thickness	lh isthmuscingulate thickness
lh lateraloccipital thickness	lh lateralorbitofrontal thickness	lh lingual thickness
lh medialorbitofrontal thickness	lh middletemporal thickness	lh parahippocampal thickness
lh paracentral thickness	lh parsopercularis thickness	lh parsorbitalis thickness
lh parstriangularis thickness	lh pericalcarine thickness	lh postcentral thickness
lh posteriorcingulate thickness	lh precentral thickness	lh precuneus thickness
lh rostralanteriorcingulate thickness	lh rostralmiddlefrontal thickness	lh superiorfrontal thickness
lh superiorparietal thickness	lh superiortemporal thickness	lh supramarginal thickness
lh frontalpole thickness	lh temporalpole thickness	lh transversetemporal thickness
lh insula thickness	lh MeanThickness thickness	rh bankssts thickness
rh caudalanteriorcingulate thickness	rh caudalmiddlefrontal thickness	rh cuneus thickness
rh entorhinal thickness	rh fusiform thickness	rh inferiorparietal thickness
rh inferiortemporal thickness	rh isthmuscingulate thickness	rh lateraloccipital thickness
rh lateralorbitofrontal thickness	rh lingual thickness	rh medialorbitofrontal thickness
rh middletemporal thickness	rh parahippocampal thickness	rh paracentral thickness
rh parsopercularis thickness	rh parsorbitalis thickness	rh parstriangularis thickness
rh pericalcarine thickness	rh postcentral thickness	rh posteriorcingulate thickness
rh precentral thickness	rh precuneus thickness	rh rostralanteriorcingulate thickness
rh rostralmiddlefrontal thickness	rh superiorfrontal thickness	rh superiorparietal thickness
rh superiortemporal thickness	rh supramarginal thickness	rh frontalpole thickness
rh temporalpole thickness	rh transversetemporal thickness	rh insula thickness
Left-Cerebellum-White-Matter	Left-Cerebellum-Cortex	rh MeanThickness thickness
Left-Thalamus-Proper	Left-Caudate	Left-Putamen
Left-Pallidum	3rd-Ventricle	4th-Ventricle
Brain-Stem	Left-Hippocampus	Left-Amygdala
CSF	Left-Accumbens-area	Left-VentralDC
Left-vessel	Right-Cerebellum-White-Matter	Right-Cerebellum-Cortex
Right-Thalamus-Proper	Right-Caudate	Right-Putamen
Right-Pallidum	Right-Hippocampus	Right-Amygdala
Right-Accumbens-area	Right-VentralDC	Right-vessel
CC Posterior	CC Mid Posterior	CC Central
CC Mid Anterior	CC Anterior	rhCortexVol
CortexVol	lhCerebralWhiteMatterVol	rhCerebralWhiteMatterVol
CerebralWhiteMatterVol	SubCortGrayVol	TotalGrayVol
SupraTentorialVol	SupraTentorialVolNotVent	SupraTentorialVolNotVentVox
MaskVol	BrainSegVol-to-eTIV	MaskVol-to-eTIV
EstimatedTotalIntraCranialVol		

---



Figure S1: Model counts for the different distributions for one single repetition over the different generations. While **Left** shows the model count for the normal data distribution, **Right** illustrates the model counts for the uniform distribution. Using both distributions, the most common models explored by TPOT are Random Forrest Regression, Extra Tree Regressors and Elastic Nets.